

## THE EFFECT OF FLUID-SATURATION ON MECHANICAL BEHAVIOR OF THE COATING–SUBSTRATE SYSTEM UNDER CONTACT LOADING

A. Yu. Smolin and G. M. Eremina

UDC 539.4.019:004.94

*The influence of the fluid saturation of a porous coating on the mechanical properties of the coating and the entire coating-substrate system is addressed. An important practical application is targeted as the wear-resistant coatings of endoprostheses of major human joints. Based on the method of movable cellular automata, a 3D-model of the mechanical behavior of a porous fluid-saturated coating on a titanium substrate is constructed. Using this model, the influence of fluid-saturation of the surface-layer of a ceramic coating on the mechanical characteristics of the coating-substrate system is studied numerically. The simulation results demonstrate that the presence of fluid in a thin surface layer of the coating can strongly affect the mechanical response of the entire coating-substrate system under sufficiently high rates of the local contact loading. In particular, the calculations without taking the fluid into account give overestimated values of strength and hardness of the coated materials under the wetting conditions. A simulation of scratching demonstrates that the material with a fluid-saturated surface layer is more stable to wear.*

**Keywords:** fluid-saturated coatings, poroelasticity, contact loading, strength, hardness, simulation, method of movable cellular automata.

### INTRODUCTION

Solid porous materials saturated with fluid are quite common in the nature, living organisms and engineering. These are primarily geomedia, including oil reserves, bone tissues, mollusk shells, various coatings, filters, foundations, etc. It is well known that these materials exhibit a non-linear deformation behavior in the cases where the solid framework porosity is permeable, which is due to fluid redistribution inside the solid under mechanical stresses. Commonly, the peculiarities of deformation of such media are studied under the conditions of constrained compression [1, 2].

In the present study we address some special aspects of mechanical behavior of a fluid-saturated porous surface layer during (local) contact loading. The practical importance of this task is primarily relevant to the use of hardening coatings in the friction units of endoprostheses of human hip and knee joints. The most common of them are metallic endoprostheses fabricated from titanium alloys; they however are subjected to rapid wear. To reduce fast wearing, they are coated with, for instance, TiN. In the course of coating deposition, pores are formed in the coating and their volume fraction can be as high as 20 % [3, 4]. After the implant is introduced into the human body, the biological fluids start penetrating into the implant through the external coating surface, which gives rise to the changes in its physical-mechanical properties.

It is impossible to investigate *in vivo* the peculiarities of the coating saturated with a biological fluid. It is hard to study this material by traditional mechanical testing methods, since it exists in the form of a coating only. Therefore,

---

Institute of Strength Physics and Materials Science of the Siberian Branch of the Russian Academy of Sciences, Tomsk, Russia, e-mail: asmolin@ispms.ru; anikeeva@ispms.ru. Translated from *Izvestiya Vysshikh Uchebnykh Zavedenii, Fizika*, No. 9, pp. 80–85, September, 2020. Original article submitted February 12, 2020.

TABLE 1. Physical-Mechanical Properties of the Porous Ceramic Coating

Density $\rho$ , kg/m <sup>3</sup>	Young modulus $E$ , GPa	Poisson's ratio $\nu$	Ultimate tensile strength $\sigma_{UTS}$ , GPa	Porosity $\phi$
5220	320	0.30	2.5	0.1

TABLE 2. Physical-Mechanical Properties of the Ti<sub>6</sub>Al<sub>4</sub>V Titanium Alloy

Density $\rho$ , kg/m <sup>3</sup>	Young modulus $E$ , GPa	Poisson's ratio $\nu$	Yield stress $\sigma_{y2}$ , GPa	Ultimate tensile strength $\sigma_{UTS}$ , GPa
4420	184	0.27	1.0	1.1

in this work we use the method of computer simulation, which has proven to be quite useful and reliable in finding solutions to such problems [5–7]. We study the mechanical behavior of the coating-substrate system using numerical experiments on local loading of a fluid-saturated coating.

This study aims at identifying the deformation features of the coating-substrate system associated with the presence of a fluid inside the surface layer of the hardening TiN coating formed on a titanium alloy substrate in the cases of such contact loading types as three-point bending, indentation, and scratching.

## 1. SIMULATION PROCEDURE AND MATERIAL BEHAVIOR MODEL

In this study we used the model of a poroelastic fluid-saturated medium, which was implemented in the methods of movable cellular automata (MCA) [8, 9] and hybrid cellular automata (HCA) [10, 11]. The simulated material was treated as an ensemble of discrete elements (cellular automata) interacting among themselves according to certain rules making it possible to describe its deformation behavior as an isotropic elastoplastic or poroelastic solid within a discrete approach. The motion of this ensemble of elements is described by the Newton–Euler equations; their mechanical interaction is the many-body interaction, which allows simulating consolidated solids [9]. The main advantage of this method for solving our tasks is its potential of an explicit simulation of fracture and an implicit inclusion of fluid inside the pores into account (in the frame of the poroelasticity model). The basis for calculating the deformation of a fluid-saturated material consists in the decomposition of the problem into to sub-problems: 1) a description of the mechanical behavior of a solid (porous medium skeleton) including the fluid pressure inside the pores into account and 2) a description of the fluid transfer in the filtration volume of interconnecting pores presented in an implicit manner [11].

The mechanical characteristics of the coating material were set in accordance with the literature data [4] and are listed in Table 1. The mechanical properties of the biological fluid corresponded to those of salt water: bulk modulus ( $K_f$ ) – 2.4 GPa and density – 1000 kg/m<sup>3</sup>.

The coating is formed on a Ti<sub>6</sub>Al<sub>4</sub>V titanium alloy substrate, which was treated as an elastoplastic material; its properties are listed in Table 2.

## 2. SIMULATION RESULTS AND DISCUSSION

### 2.1. Uniaxial compression

During simulation of uniaxial compression the sample was shaped as a cube. The load was applied by setting equal velocities in the vertical direction to the upper layer of the sample automata, with their lower layer being rigidly fixed. In the initial stage, the motion velocity of the upper layer automata was gradually increasing from 0 to 1 m/s and then remained constant. This scheme was used to rule out the artificial dynamic effects and to ensure a rapid transition of the sample deformation processes to a quasi-stationary mode. We investigated ‘dry’ and fluid-saturated samples.

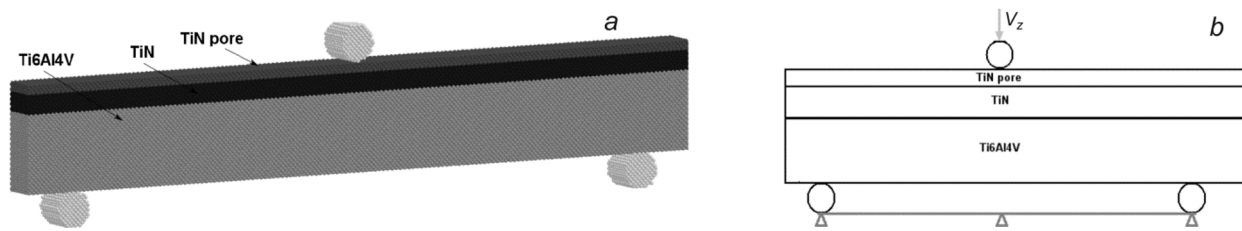


Fig. 1. Model of three-point bending of a sample with a porous surface layer of the coating (a) and its loading schematics (b).

An analysis of the results obtained demonstrated that the dry model sample possesses the highest strength, which implies a possible change of the mechanical properties of a porous TiN coating upon its interaction with a fluid.

Fluid-saturated media are quite sensitive to the loading rate; therefore in the next stage we studied the effect of the strain rate on the strength characteristics of a porous TiN coating. An analysis of the results showed that the strength-strain rate dependence is described by a sigmoid function, similarly to the results reported in [12]. Then we experimented with the influence of permeability on the effective mechanical characteristics of the fluid-saturated model sample. Similarly to [2, 12] it has been shown that the strength of a fluid-saturated material is determined by the balance of two competing processes: 1) deformation of the rigid frame, ensuring a compression of the pore space and the respective increase of the pore fluid pressure; 2) outflow/leakage of the interstitial fluid through the side surface, resulting in a reverse effect of the pore pressure decrease.

## 2.2. Three-point bending

During three-point bending simulations, the model sample represented a parallelepiped measuring  $2.14 \times 6.44 \times 42.00$  mm, which was made up of a titanium substrate and a 1.9 mm-thick TiNi coating (Fig. 1a). The upper surface layer of the coating 0.6 mm in thickness denoted as a 'TiN pore' in Fig. 1a, was thought to be porous and fluid saturated. The size of an automaton was 0.19 mm.

Loading was set by the downward motion of the indenter at a velocity of  $V_z = 1$  m/s (Fig. 1b). Using the simulation results, we obtained the curves of the bending stress dependence on time. The value of stress under bending was calculated via the following formula:

$$\sigma = \frac{3F_z l}{bh^2}, \quad (1)$$

where  $F_z$  is the force acting on the upper cylinder,  $l = 36$  mm is the distance between the supports,  $h = 6.44$  mm is the sample height, and  $b = 2.14$  mm is its width.

We addressed the effects of the fluid contained in the coating surface layer. The results demonstrated that the bending strength of the dry sample is 5% higher than that of the fluid-saturated sample (Curves 2 and 4 in Fig. 2). This circumstance is attributed to the elevated compressive stresses in the area under the indenter due to a contribution from the fluid pressure in the surface layer of coating.

Further we studied the influence of the loading rate on the values of the bending strength of the coating–substrate system. The loading rate  $V_z$  was varied from 0.5 to 2 m/s. The results obtained indicate a 10% increase in the bending strength with a four-fold increase in the loading rate (Fig. 2). This effect is accounted for by the fact that at low loading rates the fluid contained in the surface layer is redistributed from the site of contact loading to the periphery. At high loading rates, the fluid fails to redistribute and exerts an addition local pressure on the frame, resulting in crack nucleation.

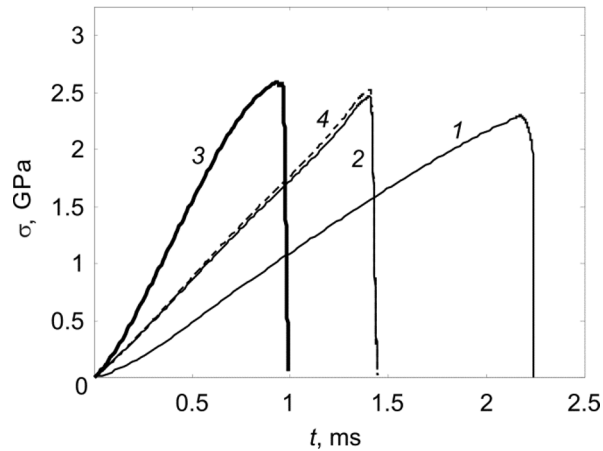


Fig. 2. Dependence of bending stress on time for model samples with dry (Curve 4) and fluid-saturated surface layer of the coating at different loading rates: 0.5 (Curve 1), 1 (Curves 2, 4) and 2 m/s (Curve 3).

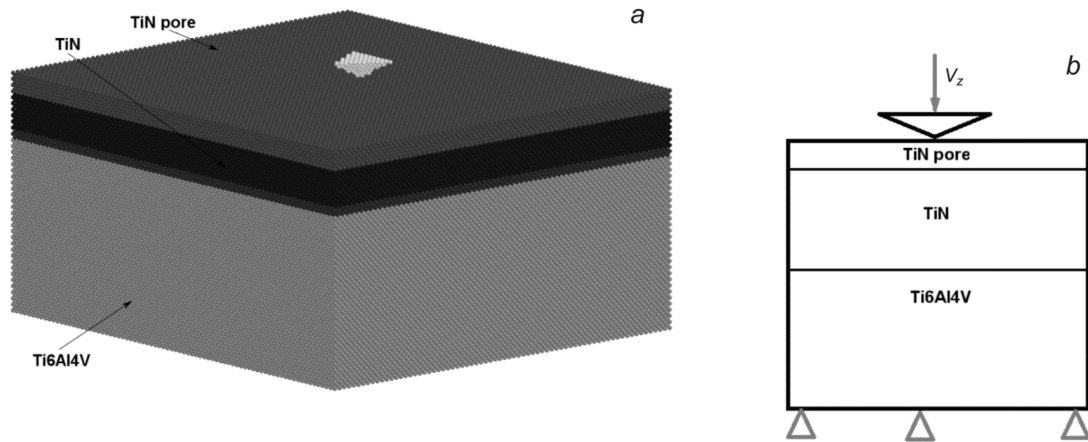


Fig. 3. Model of indentation of a system with a coating, presented as an automaton packing (a), and the loading schematics (b).

### 2.3. Instrumented indentation

The model sample was a parallelepiped with the base of  $7.5 \times 7.5$  mm and the height of 5.4 mm; it consisted of a titanium substrate and a 1.5 mm-thick TiN coating, whose upper layer, 0.3 mm in thickness, was porous and saturated with fluid (Fig. 3a). The indenter was set as a non-deformable Berkovich pyramid. The loading process was imitated by setting equal velocity of  $V_z = 1$  m/s to the indenter automata in the vertical direction (Fig. 3b).

Based on the simulation results, we constructed the curves of dependence for the hardness versus the indenter penetration depth (Fig. 4a). The resulting data suggest that the hardness in the case of indentation of the coating – substrate system with the surface layer without any fluid is higher than that in the fluid-saturated case. The largest difference is observed at small indentation depths not exceeding the thickness of the fluid-saturated surface layer.

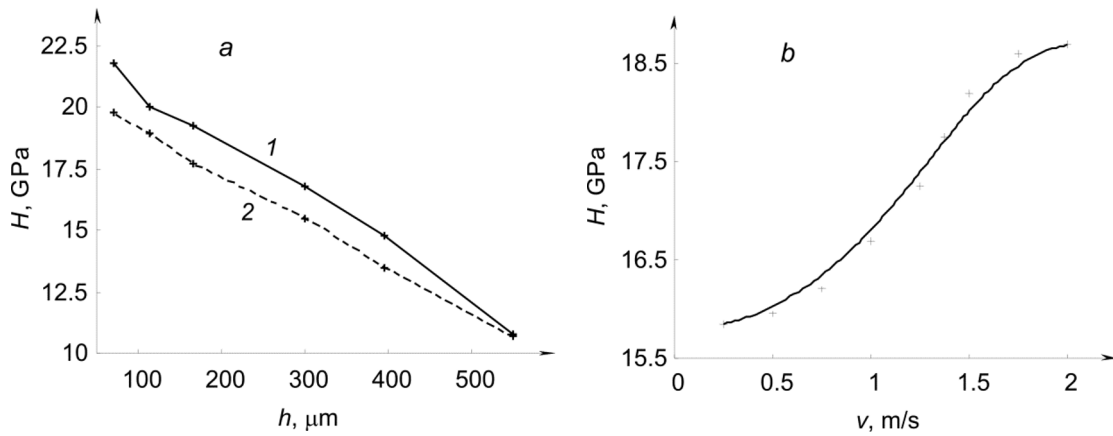


Fig. 4. Dependence of the hardness on the indenter penetration depths for the samples with dry and fluid-saturated surface layers (a) and on the loading rate for a fluid-saturated coating (b).

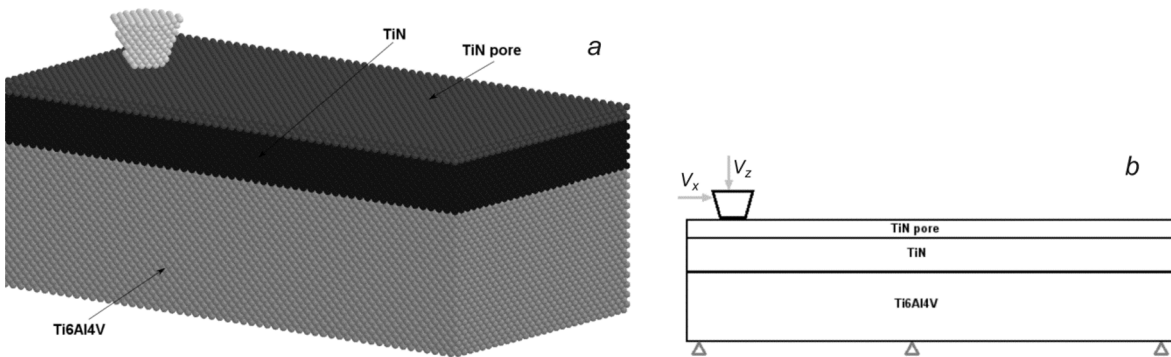


Fig. 5. Model of scratching of the system with a coating, presented as automaton packing (a), and the loading schematics (b).

It is well known that a fluid-saturated material behaves as a soft viscoelastic material, which gives rise to an error in determination of the elastic modulus and hardness in accordance with the standard procedures. A correct approach for such system is the indentation with a time delay [13, 14]. Therefore, further the mechanical behavior of the system with a fluid-saturated layer was examined in terms of its sensitivity to the loading rate. The indentation depth was 0.15 mm. We have found out that the hardness of the fluid-saturated surface layer increases nonlinearly with the loading rate, and the curve of this dependence represents a sigmoid function (Fig. 4b).

## 2.4. Instrumented scratching

The tribological characteristics of the fluid-saturated surface layer of the TiNi coating material were studied using a numerical experiment on scratching (scratch hardness testing). The counter body was a conical non-deformable indenter (Fig. 5a) immersed in a vertical position to a specified depth, which was then moved in the horizontal direction across the entire sample (Fig. 5b).

Based on the results of scratch hardness tests, we identified three stages of the coating fracture. In the first stage, the material undergoes cracking, characterized by the first peaks in the curve of time dependence of resistance to indenter motion (Fig. 6). In the case of the unsaturated surface layer, cracking develops at a force of 12 mN (Fig. 6a),

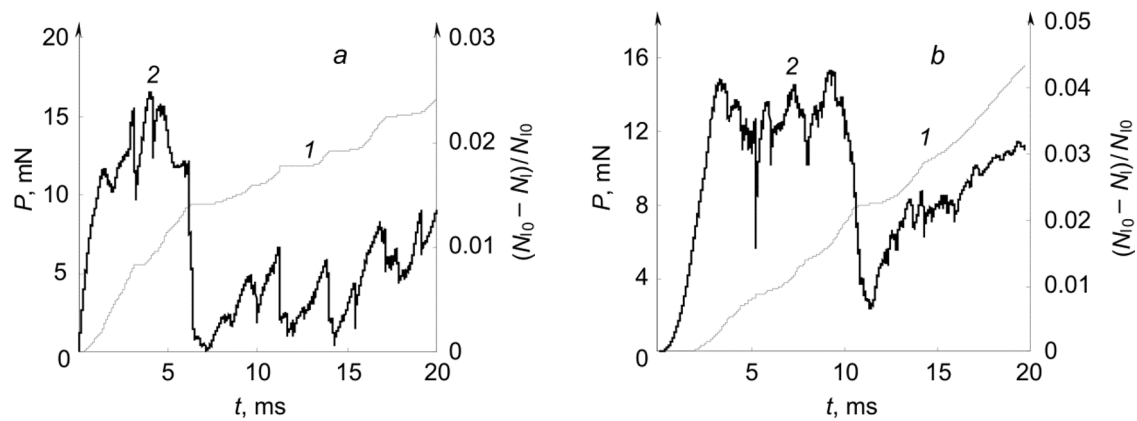


Fig. 6. Time dependence of the relative number of unbonded automata (Curve 1) and the force (Curve 2) acting on the counter body from the sample with the dry (a) and fluid-saturated (b) surface layers.

while in the case of the fluid-saturated surface layer – at 15 mN (Fig. 6b). Afterwards, there is a stage of a local delamination of the coating, which is characterized by a plateau in the resistance force vs. time curve. For the model sample with dry and fluid-saturated layers, local delamination occurs at an equal force of 15.5 mN, while in the case of the fluid-saturated coating this stage is longer, which suggests a higher wear resistance of the latter coating.

It should be noted that in the case of the dry surface layer cracking is characterized by a combination of interconnected microcracks and propagates predominantly into the bulk of the material; the area of the cracking zone on the surface corresponds to the area of the indenter-contact spot. In the case of the fluid-saturated surface layer, cracking is localized in the subsurface layer of the coating and the cracking zone area on the material surface is larger than that of the contact spot.

## SUMMARY

The numerical investigations of the effect of saturation of the surface layer of a ceramic coating with a fluid on the mechanical characteristics of the coating–substrate system have been performed. Relying on the results obtained, a conclusion can be drawn that the presence of a fluid in the thin surface layer can essentially affect the mechanical response of the entire coating–substrate system under high loading rates. It has been found out that the calculations not including the fluid into consideration give rise to overestimated values of strength and hardness of the coated materials under wetting conditions. In friction, the material with a fluid-saturated surface layer is more resistant to crack formation and wear.

This study was performed in accordance with the State Research Assignment for the ISPMS SB RAS.

## REFERENCES

1. K. S. Basniev, N. M. Dmitriev, G. V. Chilingar, *et al.*, *Mechanics of Fluid Flow*, Wiley (2012).
2. E. V. Shilko, A. V. Dimaki, and S. G. Psakhie, *Sci. Rep.*, **8**, 1428 (2018). <https://doi.org/10.1038/s41598-018-19843-8>.
3. Y. M. Chen, G. P. Yu, and J. H. Huang, *Surf. Coat. Techn.*, **150**, 309 (2002). [https://doi.org/10.1016/S0257-8972\(01\)01528-6](https://doi.org/10.1016/S0257-8972(01)01528-6).
4. B. J. McEntire, B. S. Bal, M. N. Rahaman, *et al.*, *J. Eur. Ceram. Soc.*, **35**, 4327 (2015). <https://doi.org/10.1016/j.jeurceramsoc.2015.07.034>.

5. D. S. Kryzhevich, K. P. Zolnikov, and A. V. Korchuganov, *Comput. Mater. Sci.*, **153**, 445 (2018). <https://doi.org/10.1016/j.commatsci.2018.07.024>.
6. A. I. Dmitriev, A. Y. Nikonov, A. E. Filippov, *et al.*, *Phys. Mesomech.*, **21**, 419 (2018). <https://doi.org/10.1134/S1029959918050065>.
7. W. Österle, A. I. Dmitriev, T. Gradt, *et al.*, *Tribol. Int.*, **88**, 126 (2015). <https://doi.org/10.1016/j.triboint.2015.03.006>.
8. A. Yu. Smolin, E. V. Shilko, S. V. Astafurov, *et al.*, *Def. Techn.*, **14**, 643 (2018). <https://doi.org/10.1016/j.dt.2018.09.003>.
9. E. V. Shilko, S. G. Psakhie, S. G., Schmauder S., *et al.*, *Comp. Mater. Sci.*, **102**, 267 (2015). <https://doi.org/10.1016/j.commatsci.2015.02.026>.
10. S. Zavsek, A. V. Dimaki, A. I. Dmitriev, *et al.*, *Phys. Mesomech.*, **1**, 42 (2013). <https://doi.org/10.1134/S1029959913010050>.
11. S. G. Psakhie, A. V. Dimaki, E. V. Shilko, *et al.*, *Int. J. Num. Meth. Eng.*, **106**, 623 (2016). <https://doi.org/10.1002/nme.5134>.
12. E. V. Shilko, A. V. Dimaki, A. Yu. Smolin, *et al.*, *Proc. Struct. Integrity*, **13**, 1508 (2018). <https://doi.org/10.1016/j.prostr.2018.12.309>.
13. J. A. Wahlquist, F. W. DelRio, M. A. Randolph, *et al.*, *Acta Biomater.*, **64**, 41 (2017). <https://doi.org/10.1016/j.actbio.2017.10.003>.
14. G. M. Eremina, A. Yu. Smolin, and S. G. Psahie, *Russ. Phys. J.*, **60**, No. 12, 2169 (2018). <https://doi.org/10.1007/s11182-018-1342-5>.